A Cyber-Physical System Approach for Photovoltaic Array Monitoring and Control

S. Rao, S. Katoch, P. Turaga, A. Spanias, C. Tepedelenlioglu, R. Ayyanar, H.Braun, J. Lee, U. Shanthamallu, M. Banavar[+], D. Srinivasan[++]
SenSIP Center, School of ECEE, Arizona State University, + ECE, Clarkson University, ++Poundra Inc.

***Abstract*— In this paper, we describe a Cyber-Physical system approach to Photovoltaic (PV) array control. A machine learning and computer vision framework is proposed for improving the reliability of utility scale PV arrays by leveraging video analysis of local skyline imagery, customized machine learning methods for fault detection, and monitoring devices that sense data and actuate at each individual panel. Our approach promises to improve efficiency in renewable energy systems using cyber-enabled sensory analysis and fusion.**

I. Introduction

The efficiency of solar energy farms requires detailed analytics and information on each panel regarding voltage, current, temperature and irradiance. We describe machine learning and computer vision approaches for improving the efficiency and reliability of utility scale solar arrays. Efficiency improvements are accomplished through prediction of complex dynamical system parameters using sensors and sensor fusion. The methods presented in this paper will be implemented on state of the art testbed shown in Figure 1. This testbed was developed by the Sensor Signal and Information Processing (SenSIP) Center and involves an 18kW array of 104 panels. Cyber-physical methods that include imaging and machine learning algorithms for shading prediction and fault detection are being developed to improve efficiency. These methods will be validated on the SenSIP Solar facility.

Figure 1. The SenSIP 18kw (104 panel) experimental facility established at ASU with industry collaborators [1].

Camera and satellite sensing of skyline features as well as parameter sensing at each panel provides information for fault detection and power output optimization through sensor fusion and appropriate actuator programming. Machine learning and fusion enables us to implement robust shading prediction. The co-authors have worked with Poundra and Energy Wireless to develop and integrate smart monitoring devices (SMDs) equipped with voltage, current, and irradiance sensing for fault detection. Prior work by this team produced signal processing algorithms for PV monitoring reported in [1-4].

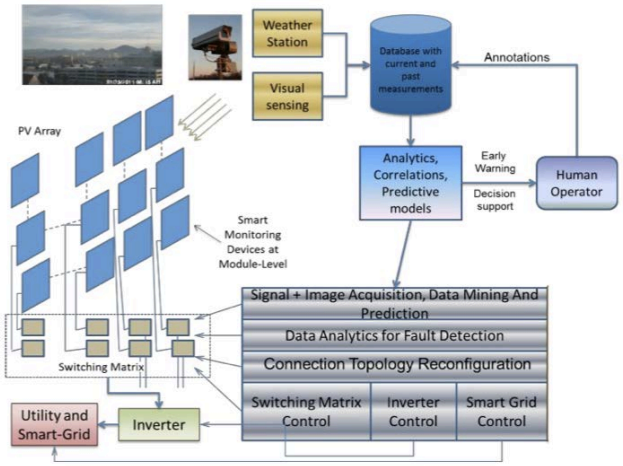

Figure 2. Networked PV Array Concept enabling: a) weather feature correlations, b) local shading prediction, c) decision support, and d) fault detection.

Efficiency improvements of up to 4% were documented using circuit simulation models [2-5]. Our estimates show that efficiency improvements up to 10% are possible using shading prediction, customized sensor fusion and machine learning algorithms for fault detection. The introduction of cameras and new imaging algorithms enables short and long-term prediction of cloud and shading patterns that will be integrated in the overall monitoring and control system. Cloud movement prediction enables new strategies for power grid control, array topology reconfiguration, and control of inverter transients. New machine learning methods that employ recently developed divergence measures [6] will reduce uncertainty in fault detection and enable improved monitoring and control of utility scale remote solar sites. The SMDs have relays that enable reconfiguration of connection topologies.

A utility-scale PV array consists of solar panels that are connected in series, forming strings, which are in turn connected in parallel. The DC output of the array is converted to AC using inverters. Shading, weather patterns and temperature can severely affect power output. To minimize these effects, individual panel current-voltage (I-V) measurements, weather information [7-13], and imaging data are essential. Moreover, controlling the power output is possible through matrix switching (i.e., changing array topology enabled by SMD relays [1]) of PV panels allowing for

different interconnection options. We optimize utility scale PV array systems by exploiting the measured I-V, imaging, and weather data. The smart monitoring devices connected to each PV panel collect the individual panel metrics (current, voltage, and temperature) periodically (about every 8 seconds). The cameras provide updates at a rate of 20-30 frames per second.

The algorithmic and image/data analysis unit are equipped with various state of the art algorithms for imaging, data mining and prediction that identify and track various important time-varying events and patterns. The algorithms operate on PV array measurements and on parametric models to detect and remedy faults using SMD panel switching (Fig. 2) or bypassing if necessary [1]. Reference [1] explains how SMD relays operate upon command to reconfigure the connection topology. The development of image and video-based algorithms for modeling and prediction of skyline features, and the study of the underlying mathematical structures of the model parameters differentiate this paper from the previous efforts of the team [2].

II. Dynamic Models for Skyline Videos

Let *f(t)* be a sequence of texture and color features extracted from a short video of the skyline indexed by time. The linear dynamical model [15-18] parametrizes the evolution of the features using the following equations:

$$f(t) = Cz(t) + w(t) \qquad w(t) \sim \mathcal{N}(0, R) \qquad (1)$$

$$z(t+1) = Az(t) + v(t), \qquad v(t) \sim \mathcal{N}(0, Q) \qquad (2)$$

where, $z \in \mathbb{R}^d$ is the hidden state vector, $A \in \mathbb{R}^{d*d}$, the transition matrix and $C \in \mathbb{R}^{p*d}$, the measurement matrix. The function $f \in \mathbb{R}^p$ represents the observed features while w and v are noise components modeled as normal with zero mean and covariances $R \in \mathbb{R}^{p*p}$ and $Q \in \mathbb{R}^{d*d}$ respectively. For the LDS model of (2), starting from an initial condition z (0), it can be shown that the expected observation sequence derived from a time-invariant model $M = (A, C)$ lies in the column space of the extended observability matrix given by

$O_\infty^T = [C^T, (CA)^T, (CA^2)^T, \ldots, (CA^n)^T, \ldots]$. In practice, we truncate the extended observability matrix, $O_m^T = [C^T, (CA)^T, (CA^2)^T, \ldots, (CA^{m-1})^T, \ldots]$ and build our additional analysis on the truncated version. The truncation does not introduce error in our case, since beyond a few concatenations the column rank of the matrix reaches its maximum value (if the system is observable). The column space of this matrix is a d- dimensional subspace of $\mathbb{R}^{mp}$, where d is the dimension of the state-space z and is typically of the order of 5-10. The linear dynamical model is a rich model for representing the dynamic variations of observed texture patterns. The parameters of the dynamical model are best viewed as subspaces formed by the columns of the observability matrix. Formally, the set of all d-dimensional linear subspaces of $\mathbb{R}^n$ is called the Grassmann manifold which will be denoted as $\mathcal{G}_{n,d}$ [14]. In this paper, we are interested in developing theoretically well-grounded and computational efficient algorithms to map the LDS parameters to attributes describing skyline features from the imagery. This requires us to consider the underlying geometric properties of the parameter-space: which in our case is the Grassmannian. In previous work, we described computing statistical models over the Grassmann manifold for various image based applications [14]. We will further build upon these insights in this paper to extract long term robust correlations between the observed imagery and PV circuit characteristics.

A. Riemannian geometric interpretation of dynamic model parameters

Since we are interested in performing various statistical correlation analyses with the estimated skyline dynamical models, we need to first consider the challenges in performing a standard multivariate statistical analysis if the underlying state space is non-Euclidean. These analyses require the use of tangent-spaces and exponential/inverse exponential maps. In previous work, we have elaborated on the use of Riemannian geometric concepts such as exponential maps, inverse exponential maps etc. which will be brought to bear upon the current task [14,21,22]. We illustrate the notion of the exponential map in the Figure 3.

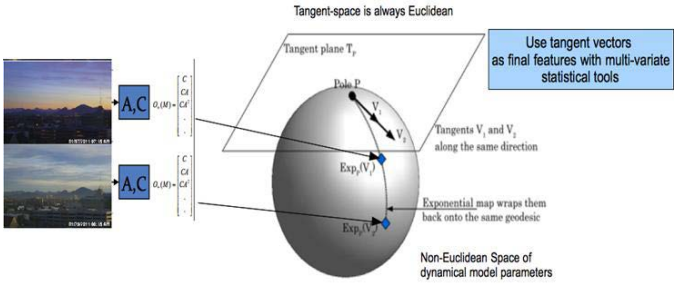

Figure 3. This figure illustrates exponential and inverse-exponential maps. These mappings extend the wealth of multivariate statistical machine learning algorithms to our general manifolds. The tangent vectors represent the final features that will be used in conjunction with other machine learning tools for mapping video features to skyline attributes.

These tools allow one to locally linearize the parameter-space, and employ classical multi-variate statistical tools, such as computing probability densities from sample data and regression to relevant attributes. Below we describe the specific forms of these expressions for the special case of the Grassmann manifold, described in more detail in [14]. A Grassmann manifold [24,25] is the set of all d-dimensional subspaces of $\mathbb{R}^n$. Here we are interested in d-dimensional subspaces and not in one particular basis. An equivalence class is given by, $[O]_b = \{O\phi_b\ (V_1, V_2) \mid V_1 \in SO(d), V_2 \in SO\ (n - d)\}$, and the set of all such equivalence classes is $\mathcal{G}n,d$. Notationally, $\mathcal{G}n$,d can also be denoted as simply $SO(n)/(SO(d) \times SO\ (n - d))$. To utilize standard multi-variate statistical models for correlation extraction, we need to 'linearize' the curved space using the tangent-space structure of the underlying manifold. For any other point $[U] \in \mathcal{G}n$,d , let $O \in SO$(n) be a matrix such that $U = O^T J$. Then, the tangent space at $[U]$ is given by $T_{[U]}(\mathcal{G}n,d) = \{O^T G \mid G \in T_{[J]}(\mathcal{G}n,d)\}$. On $\mathcal{S}n$,d and

$\mathcal{G}n$,d , the exponential map is given by, $O^T\ [\ C; B^T] \equiv O^T\ A\mathcal{J} \mapsto O^T \exp(A)\ J$, where A takes an appropriate structure for each case. The expression for inverse exponential map is not available analytically for these manifolds and is computed numerically. These tangent vectors themselves can be used as inputs to standard multivariate statistical tools or other machine learning algorithms as illustrated in Figure 3. The dimensionality of the tangent vectors is the same as the dimensionality of the manifolds; which in turn is governed by the dimensionality of our video features. We expect that the textural features extracted from the video will be high dimensional (of the order of the number of pixels in the image). Fortunately, we can reduce dimensionality of the tangent vectors via principled extensions of tools such as principal component analysis to consider the curvature of the space [19, 20]. This approach has been termed geodesic principal components in the broader community, and we will adopt such variations to reduce computational load. Shown in Figure 4, is the general framework for constructing conditional probability density functions over linear dynamical model parameters for skyline attributes such as 'clear', 'light clouds', and 'overcast'. These pdfs will be modeled as wrapped normal distributions (potentially mixtures of Normals) over the Grassmann manifold from training data, using the procedure described above. These basic building blocks will be used in the proposed framework for fault prediction.

B. Temporal prediction of dynamical systems

The classification methods of dynamic textures as described previously are effective in short durations of time, when one can assume that the dynamic texture has wide-sense statistical stationarity to further enhance prediction, we need to consider looking forward in time, and anticipating dynamical evolution. Assuming linear dynamics and wide sense stationarity is often an unrealistic assumption when faced with the task of predicting the evolution of a dynamical pattern. For long-term prediction, we consider the problem of studying the evolution using non-linear tools, which avoids making restrictive assumptions on parametric forms. The basic principle we adopt is one of reconstructing the hidden phase-space of the true dynamic system using delay embeddings.

Note here, that the dynamical system under consideration is multi-variate to begin with, since the extracted features are of the order of pixels in the image. From the reconstructed phase-space, the prediction problem is tackled using simple regression models in the phase space. This contrasts with prediction using regression models in the observation space, which is much harder due to the non-smooth properties of the observation sequence. If the phase-space reconstruction is properly achieved, the evolution in the phase space is much smoother, which will allow prediction of the next few phases. Mapping from predicted phases to expected pixel measurements can be achieved, which will allow us to use the previously developed linear models for classification into one of several shading categories.

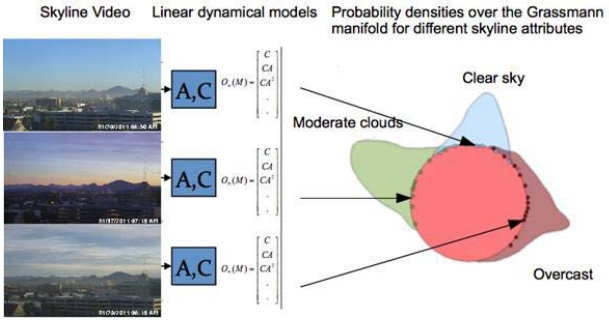

Figure 4. Illustration of proposed algorithm for estimating conditional densities of skyline features from video measurements. Video streams are modeled as linear dynamical models, whose parameters are considered as points on a Grassmann manifold. Conditional pdfs of sky attributes are estimated using Riemannian geometric tools.

III. I-V FEATURES AND USE OF MACHINE LEARNING FOR FAULT DETECTION

Reliability is a crucial factor in a PV system. Ground faults, series and parallel arc faults, high resistance connections, soiling, and partial shadowing need to be addressed. A solar cell or panel is often modeled as a current source and a diode, with parasitic series and shunt resistance (see Figure 5).

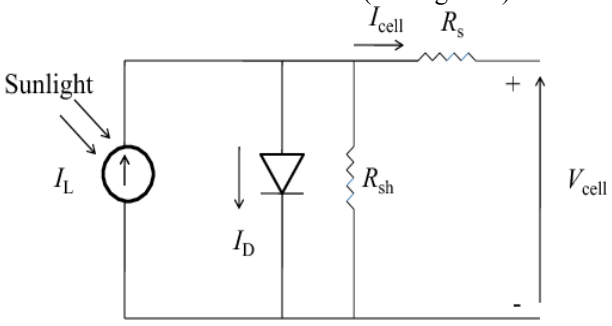

Figure 5. Circuit model for a PV module.

The I-V data in a PV array can be measured at the panel-level inexpensively. This data is useful since it can be used to build correlation models with the imaging data, and is useful in predicting possible ground faults or arc faults. The I-V characteristic is a function of temperature, incoming solar irradiance (direct and diffused), angle of incidence, and the spectrum of sunlight. The panel has an optimal operating point for maximum power. Fault detection using I-V data can be accomplished by identifying outliers in the I-V feature space. I-V measurements are typically highly correlated. Moreover, the dynamics of the I-V measurements lend themselves to predictive models.

A. Existing Approaches for fault detection

There are several articles in the literature on early fault detection in solar arrays [26-31, 33]. However, none of these techniques exploit statistical hypothesis testing algorithms. In our work [3, 4] we show that we can detect faults in individual modules using clustering algorithms. In our preliminary results, an algorithm was developed to identify underperforming panels.

B. *Using Machine Learning for Fault Detection*

Current practice is to identify faults via a human operator examining data collected at the inverter. One study identified a Mean Time to Repair (MTTR) of 19 days for a centrally monitored system of residential installations [31]. With the addition of more and higher quality data from SMDs, MTTR could be significantly reduced.

Several challenges and research opportunities are evident in the fault diagnosis and localization problems. First, of course, a system must accurately classify the PV array's condition. It must be adaptable to different array configurations without extensive data collection for each individual array. It should be able to react to the 'unknowns'--faults the system designers did not anticipate. Considering these challenges, several machine learning [43] approaches can be examined. Semi-supervised learning could allow the generation of many realistic faults from a few measured examples.

IV. Preliminary Results

A. *Temporal prediction of dynamical systems*

Given a large dataset of the observed imagery, we would like to obtain useful correlations between the proposed dynamical models, and circuit-level measurable I-V characteristics. Here, in Figure 6. , we show a simple example to demonstrate the utility of the skyline dynamical model and Riemannian geometry based computations to classify attributes of cloud and shading activity. For this experiment, we took a month-long video-log from a weather camera looking at the skyline of the Camelback Mountain in Phoenix AZ. A frame was captured once every 30 mins, though we anticipate that for early warning interventions, we may require higher capture rate. However, this data still serves as an excellent test bed to measure the usability of imagery to develop attributes for early warning. We created a small training set where we annotated a few segments as 'clear', 'moderate cloudy', and 'overcast'. This training set was used to learn a probability density function on the Grassmannian. As seen in figures 6 and 7, the scores provided to test data encode meaningful attributes. A high score implies clear skies and a low score implies overcast skies. These results are encouraging and show that one can detect such attributes from oncoming clouds and use those as early indicators of shading. To illustrate the strength of the dynamical approach on predicting transition between cloudy and non-cloudy patterns, we consider a non-linear Lyapunov exponent based approach. For the textural feature per frame, we will use Gabor filter-bank responses.

Modeling temporal dynamical evolution of these textural features using largest Lyapunov exponents, we get a spatio-temporal representation of sky videos, per feature dimension. From Figure 7, we see that largest Lyapunov exponents provide a clear distinction between clear sky and cloudy sky, with spatiotemporal modeling providing information about the transition phase between these two states.

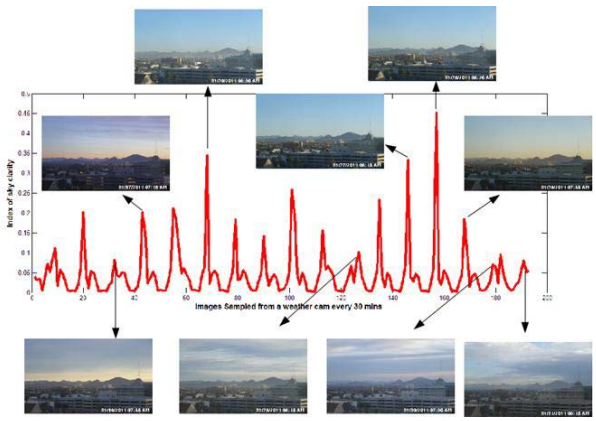

Figure 6. Image-based measures of sky-clarity, an attribute useful for predicting shading. This metric was created from dynamical models of image texture, with a manifold-based metric on dynamical model parameters. Sample images at various times show how the index separates 'clear skies' and 'hazy/cloudy skies'. Using a small network of horizon-viewing cameras it is possible to develop early warning systems.

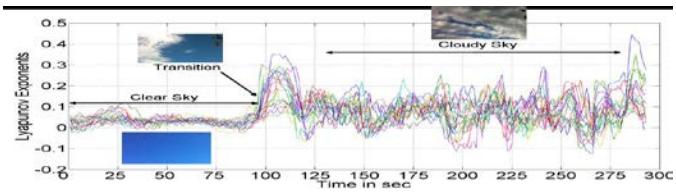

Figure 7. Spatio-temporal modeling of sky videos using GIST and largest Lyapunov exponents; with time stamps for clear sky, transition from clear-cloudy sky and cloudy sky. These transitions can be used for prediction.

B. *Minimum Covariance Determinant estimator for fault detection*

The Minimum Covariance Determinant (MCD) can estimate the center and shape of a cluster [38]. In the PV context, this algorithm could run on V-I plots across all panels. The MCD minimizes the function $det(\widehat{\boldsymbol{\Sigma}})$ over all possible subsets H of the data containing observations of H PV panels, where $\widehat{\boldsymbol{\Sigma}}$ is the sample covariance matrix of H. The output of an MCD algorithm consists of the optimal subset of panels H* and its centroid is μ_{h^*} and covariance matrix $\sum^*$. μ_{h^*} and $\sum^*$ may be used to form a distance metric $d(M) = \sqrt{(M - \mu_{h^*})^T \sum^* (M - \mu_{h^*})}$ which measures the extent to which a measurement is an outlier.

The FAST-MCD algorithm [39] can determine approximate results with reduced complexity by iteratively modifying the subset of h points such that its covariance determinant decreases with each iteration, rather than testing every possible subset. In preliminary simulations using only voltage and current data and (temporarily) excluding temperature measurements, the MCD-based detection method delivered reliable results when applied to simulated arc and ground faults, as shown in Figures 8 and 9. Figure 9 shows a scatter plot of the panel voltages and currents during an arc event where the faulty panel is resolved to be outside the cluster of functioning panels. These preliminary

simulations with synthetic data indicate that most faults can be reliably detected.

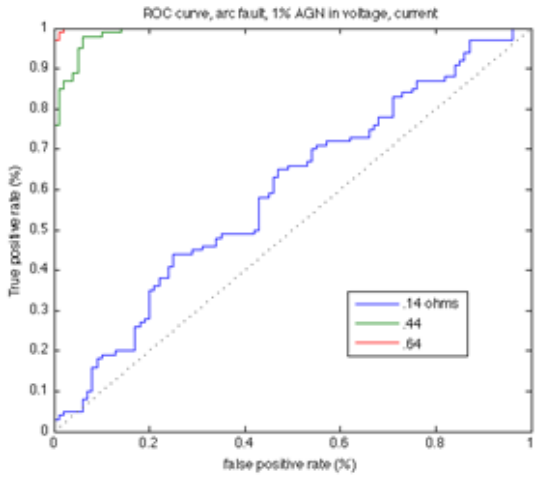

Figure 8. ROC curves for series arc fault.

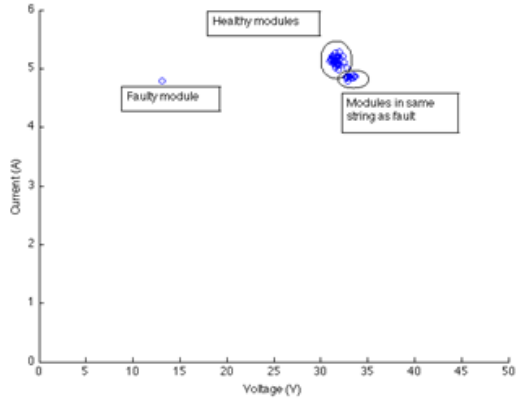

Figure 9. Scatter Plot under arc fault.

C. *Preliminary Results Using Gaussian Mixture Models:*

Machine learning algorithms have been successful in several signal and image processing applications [34-35]. The utility of machine learning tools and Internet-of-Things (IoT) topologies in renewable energy has been reported before in [44-46]. To demonstrate the feasibility of applying machine learning for fault detection, we started with a simple k-means algorithm with results reported in [1]. However, with the use of probabilistic models rather than hard boundaries, we can obtain better clustering results [35,43]. As an initial step, we explore the use of Gaussian Mixture Models trained with Expectation Maximization (EM).

The result in Figure 10 shows the implementation of fault detection using Gaussian Mixture Models. Simulated fault data were obtained using the UW-Madison PV model and a SPICE circuit simulation [21-23]. The dataset was gathered under normal conditions. A cluster for each panel was formed. Two clusters were randomly initialized. For the training of clusters, we use the EM algorithm as it has shown to perform well in clustering applications [35]. The difference in the simulated faulty panel and normally working panel are seen from two different clusters in Figure 10. The normally functioning panel has cluster points which are compact while the scattered cluster points indicate the simulated faulty panel.

Further statistical analysis is needed to develop a better understanding of clustering patterns. Customized machine learning methods that use divergence measures [6] to improve clustering in cases where there are overlaps.

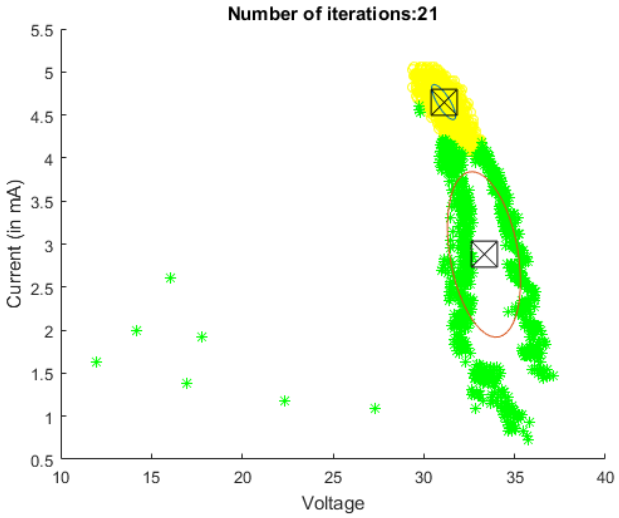

Figure 10. Clustering using GMM. Training forms clusters of normal and simulated fault PV data.

V. Conclusion

We addressed the problem of PV array monitoring and control using advanced imaging and machine learning algorithms. We proposed integration of machine learning, image processing and optimization techniques for real time monitoring of PV arrays. Preliminary results for fault detection demonstrated clustering successfully faults and our simulations with imaging prediction promise significant efficiency improvements.

Acknowledgment

This work was supported in part by the NSF CPS award 1646542 and the ASU SenSIP Center. We also appreciate the logistical support of Energy Wireless, Poundra, ASU SenSIP, ASU MTW, and ASU OKED in planning the construction of the solar panel monitoring facility.

References

[1] A. Spanias, C. Tepedelenlioglu, E. Kyriakides, D. Ramirez, S. Rao, H. Braun, J. Lee, D. Srinivasan, J. Frye, S. Koizumi, Y. Morimoto, "An 18 kW Solar Array Research Facility for Fault Detection Experiments," *Proc. 18th MELECON, Tech. Co-sponsor IEEE Region 8*, T1.SP1.12, Limassol, April 2016.

[2] H. Braun, S. T. Buddha, V. Krishnan, A. Spanias, C. Tepedelenlioglu, T. Takehara, S. Takada, T. Yeider, and M. Banavar, Signal Processing for Solar Array Monitoring, Fault Detection, and Optimization, Synthesis Lect. Power Electronics, J. Hudgins, Ed. Morgan & Claypool, vol. 3, Sep. 2012.

[3] Braun, H.; Buddha, S.T.; Krishnan, V.; Spanias, A.; Tepedelenlioglu, C.; Yeider, T.; Takehara, T.; "Signal processing for fault detection in photovoltaic arrays," *2012 IEEE International Conference on, Acoustics, Speech and Signal Processing (ICASSP),* pp.1681-1684, 25-March 2012.

[4] Buddha, S.; Braun, H.; Krishnan, V.; Tepedelenlioglu, C.; Spanias, A.; Yeider, T.; Takehara, T.; "*Signal processing for photovoltaic applications*," *IEEE ESPA*, vol., no., pp.115-118, 12-14 Jan. 2012.

[5] H. Braun, S. T. Buddha, V. Krishnan, C. Tepedelenlioglu, A. Spanias, M. Banavar, and D. Srinivasan, "Topology reconfiguration for optimization of photovoltaic array output," *Elsevier Sustainable Energy, Grids and Networks* (*SEGAN),* pp. 58-69, Vol. 6, June 2016.

[6] V. Berisha, A. Wisler, A. Hero, A. Spanias, "Empirically Estimable Classification Bounds Based on a Nonparametric Divergence Measure," IEEE *Transactions on Signal Processing,* vol. 64, no. 3, pp.580-591, Feb. 2016.

[7] Marquez, Ricardo, Hugo TC Pedro, and Carlos FM Coimbra. "Hybrid solar forecasting method uses satellite imaging and ground telemetry as inputs to ANNs." *Solar Energy*, vol. 92, pp. 176-188, June 2013.

[8] Quesada-Ruiz, S., et al. "Cloud-tracking methodology for intra-hour DNI forecasting." *Solar Energy*, vol. 102, pp. 267-275, April 2014.

[9] P. Bacher, H. Madsen, H.A. Nielsen, "Online short-term solar power forecasting," *Solar Energy*, vol. 83, no. 10, pp. 1772-1783, October 2009.

[10] M. Hassanzadeh, M. Etezadi-Amoli, M.S. Fadali, "Practical Approach for Sub-Hourly and Hourly Prediction of PV Power Output," *North American Power Symposium (NAPS)*, 2010.

[11] Chu, Yinghao, et al. "A smart image-based cloud detection system for intrahour solar irradiance forecasts." *Journal of Atmospheric and Oceanic Technology,* vol. 31.9, May 2014.

[12] L. Ciabattoni, G. Ippoliti, S. Longhi, M. Cavalletti, M. Rocchetti, "Solar Irradiation Forecasting using RBF Networks for PV Systems with Storage," *ICIT*, 2012.

[13] G.M. Tina, S. De Fiore, C. Ventura, "Analysis of forecast errors for irradiance on the horizontal plane," *Energy Conversion and Management*, vol. 64, pp. 533-540, December 2012.

[14] P. Turaga, A. Veeraraghavan, A. Srivastava, R. Chellappa "Statistical Computations on Grassmann and Stiefel Manifolds for Image and Video-Based Recognition," *IEEE Trans. Pattern Anal. Mach. Intel.* 33(11): 2273-2286 (2011).

[15] G. Doretto, A. Chiuso, Y.N. Wu, A. Soatto, "Dynamic Textures," *International Journal of Computer Vision (IJCV),* vol. 51, no. 2, pp. 91-109, 2003.

[16] S. Soatto, G. Doretto, Y.N. Wu, "Dynamic Textures," *IEEE Int.Conf. Comp. Vision*, 439-446, 2001.

[17] Antoni B. Chan, Nuno Vasconcelos: Modeling, Clustering, and Segmenting Video with Mixtures of Dynamic Textures. *IEEE Trans. Pattern Anal. Mach. Intel*, vol. 30(5), pp. 909-926, 2008.

[18] A. Srivasatava and E. Klassen, "Bayesian and geometric subspace tracking," *Advances in Applied Probability*, vol. 36, no. 1, pp. 43–56, March 2004.

[19] R. Anirudh, P. Turaga, "Geometry-based Adaptive Symbolic Approx. for Low Complexity Activity Analysis," *IEEE Transactions on Image Processing*, March 2015.

[20] R. Anirudh, V. Venkataraman, and P. Turaga. "A generalized lyapunov feature for dynamical systems on riemannian manifolds," *First Int. Workshop on Diff. Geometry in Computer Vision,* Sep 2015.

[21] D. Nguyen and B. Lehman, "Modeling and simulation of solar pv arrays under changing illumination conditions," in Computers in Power Electronics, COMPEL '06. IEEE Workshops on, pp. 295 –299, 2006.

[22] V. Quaschning and R. Hanitsch, "Numerical simulation of current-voltage characteristics of photovoltaic systems with shaded solar cells," *Solar Energy,* vol. 56, no. 6, 1996.

[23] G.D. Gregory and G.W. Scott, "The arc-fault circuit interrupter: an emerging product," *Industry Applications, IEEE Transactions on*, vol. 34, no. 5, pp. 928-933, 1998.

[24] W. Boothby, An introduction to differentiable manifolds and Riemannian geometry, Academic Press, 1975.

[25] A. Edelman, T. A. Arias, and S. T. Smith, "The geometry of algorithms with orthogonality constraints," *SIAM Journal Matrix Analysis and Application*, vol. 20, no. 2, pp. 303–353, April 1999.

[26] H. Haeberlin and M. Kaempfer, "Measurement of Damages at Bypass Diodes by Induced Voltages and Currents in PV Modules Caused by Nearby Lightning Currents with Standard Waveform," in *23rd European Photovoltaic Solar Energy Conference*, 2008.

[27] N. Bosco, "Reliability concerns associated with PV technologies," *National Renewable Energy Laboratory*, Albuquerque, 2010.

[28] L. L. Jiang and D. L. Maskell, "Automatic fault detection and diagnosis for photovoltaic systems using combined artificial neural network and analytical based methods," 2015 *International Joint Conference on Neural Networks (IJCNN), Killarney*, 2015, pp. 1-8.

[29] M. N. Akram and S. Lotfifard, "Modeling and Health Monitoring of DC Side of Photovoltaic Array," in *IEEE Transactions on Sustainable Energy*, vol. 6, no. 4, pp. 1245-1253, Oct. 2015.

[30] D. Nilsson, Fault detection in Photovoltaic Systems, Master's Thesis at KTH, 2014.

[31] A. Maish, C. Atcitty, S. Hester, D. Greenberg, D. Osborn, D. Collier, and M. Brine, "Photovoltaic system reliability," *Photovoltaic Specialists Conf. Conf. Rec 26th IEEE*, 29 1997, pp. 1049 –1054.

[32] M. Banavar, C. Tepedelenlioglu, A. Spanias, "Robust Consensus in the Presence of Impulsive Channel Noise," *IEEE Trans. on Signal Proc., Vol.* 63, pp. 2118-2129, March 2015.

[33] D.L. King, J.A. Kratochvil, and W.E. Boyson, Photovoltaic array performance model, United States, Dept. of Energy, 2004.

[34] M.G. Villalva, J.R. Gazoli, and E.R. Filho, "Comprehensive Approach to Modeling and Simulation of Photovoltaic Arrays," *IEEE Transactions on Power Electronics,* vol. 24, no. 5, pp. 1198-1208, 2009.

[35] I.V. Cadez, C.E. McLaren, P. Smyth, G.J. McLachlan, "Hierarchical Models for Screening of Iron Deficiency Anemia", *Proceedings of the International Conference on Machine Learning*, Los Gatos, 1999.

[36] J. Thiagarajan, K. Ramamurthy, P. Turaga, A. Spanias, Image Understanding Using Sparse Representations, Synthesis Lectures on Image, Video, and Multimedia Processing, Morgan & Claypool Publishers, ISBN 978-1627053594, Ed. Al Bovik, April 2014

[37] H. Song, J. J. Thiagarajan, P. Sattigeri, K. Ramamurthy, A. Spanias, 'A Deep Learning Approach to Multiple Kernel Fusion," *Proc. IEEE ICASSP 2017*, New Orleans, 2017.

[38] P. Rousseeuw, "Multivariate estimation with high breakdown point," *Mathematical statistics and applications*, vol. 8, pp. 283–297, 1985.

[39] P. J. Rousseeuw and K. v. Driessen, "A fast algorithm for the minimum covariance determinant estimator," *Technometrics*, pp. 212–223, 1999.

[40] S. Alzahrani, "Matlab Source Code an Implementation of the Expectation Maximization Algorithm v1," Sep. 2016.

[41] H. Braun, P. Turaga, A. Spanias, G. Tepedelenlioglu, 'Direct Classification from Compressively Sensed Images via Deep Boltzmann Machine," *IEEE Asilomar Conference on Signals, Systems and Computers*, Monterey, pp. 454-457, Nov. 2016.

[42] H. Song, J. Thiagarajan, K Ramamurthy, A. Spanias, P. Turaga, "Iterative Kernel Fusion for Image Classification", MLSP-L2.4, *IEEE ICASSP 2016,* Shanghai China, March 2016.

[43] U. Shanthamallu, A. Spanias, C. Tepedelenlioglu, M. Stanley, "A Brief Survey of Machine Learning Methods and their Sensor and IoT Applications," *Proceedings 8th International Conference on Information, Intelligence, Systems and Applications (IEEE IISA 2017)*, Larnaca, August 2017.

[44] A. Spanias, "Solar Energy Management as an Internet of Things (IoT) Application," *Proceedings 8th International Conference on Information, Intelligence, Systems and Applications (IEEE IISA 2017)*, Larnaca, August 2017.

[45] Opengear, 2017, Benefits Of IoT For Solar Power, http://opengear.com/articles/benefits-challenges-iot-solar-energy

[46] G. Du et al, "Based on the Internet of things a self-cleaning solar power system of the household micro-grid," *2016 Chinese Control and Decision Conference (CCDC)*, May 2016.